

UNCLASSIFIED

AD 256 927

*Reproduced
by the*

**ARMED SERVICES TECHNICAL INFORMATION AGENCY
ARLINGTON HALL STATION
ARLINGTON 12, VIRGINIA**



UNCLASSIFIED

NOTICE: When government or other drawings, specifications or other data are used for any purpose other than in connection with a definitely related government procurement operation, the U. S. Government thereby incurs no responsibility, nor any obligation whatsoever; and the fact that the Government may have formulated, furnished, or in any way supplied the said drawings, specifications, or other data is not to be regarded by implication or otherwise as in any manner licensing the holder or any other person or corporation, or conveying any rights or permission to manufacture, use or sell any patented invention that may in any way be related thereto.

256927

CATALOGED BY ASTIA
AS AD NO.

TR-905

NEUTRON DOSIMETRY USING INELASTIC SCATTERING THRESHOLD DETECTORS

John S. Ingley

258200

16 March 1961

XEROX



DIAMOND ORDNANCE FUZE LABORATORIES
ORDNANCE CORPS • DEPARTMENT OF THE ARMY

* 3.60

**DIAMOND ORDNANCE FUZE LABORATORIES
ORDNANCE CORPS WASHINGTON 25, D. C.**

**DA-5W98-09-003
ONS-5010.11.83000
DOFL Proj 23000**


TR-905

16 March 1961

NEUTRON DOSIMETRY USING INELASTIC SCATTERING THRESHOLD DETECTORS

John S. Ingley

**FOR THE COMMANDER:
APPROVED BY**


**B. M. HORTON
Chief, Laboratory 200**



Qualified requesters may obtain copies of this report from ASTIA

CONTENTS

	Page No.
ABSTRACT.	5
1. INTRODUCTION.	5
2. THEORY.	9
3. EQUIPMENT	12
4. PROCEDURE	12
5. REDUCTION AND ANALYSIS OF DATA.	16
6. CONCLUSIONS	29
7. BIBLIOGRAPHY.	29

ABSTRACT

Employing a new threshold detector that utilizes the inelastic scattering reaction to the isomeric state of Ba^{137} , the time-integrated neutron flux above 1.9 Mev was measured in the General Atomic Triga reactor. The values compare favorably with those extrapolated from measurements of the flux above 2.9 Mev given by the standard sulfur pellet method, and evidence thus far indicates that the new method may provide a whole new series of threshold detectors.

1. INTRODUCTION

An important phase of neutron radiation damage experimentation is the measurement of the neutron flux that produces the damage. The most versatile flux measurement method available today is the foil activation method. In this method, the activation produced in various materials by the neutron flux is used to measure the flux in specific energy regions. Three types of activation foils are currently in use--thermal, resonance, and threshold. Thermal foils are used to measure the integrated energy-dependent flux in the thermal region (0 to ~ 0.4 ev). Resonance foil are used to measure the energy-dependent flux at specific energies by means of large, isolated resonances in the neutron absorption cross section. Threshold foils are used to measure the integrated energy-dependent flux above a specific energy. At present, thermal and resonance foils can be used to measure the energy-dependent flux up to 10 Kev, while threshold foils can be used to determine the energy-dependent flux above 600 Kev. This leaves a considerable gap, between 10 and 600 Kev, where no measurements can be made at the present time by foil techniques.

A search through the neutron cross-section tables immediately makes it apparent that there are no large, narrow, isolated resonances in the energy range of interest. The main reason for this is that the energy levels in the intermediate compound nuclei are very close together for energies of 100 Kev or more. Thus we are forced to rely on threshold detectors for any measurements in this region.

A threshold reaction is one that has a negligible or zero cross section below a certain energy. For example, if a given (n,p) reaction is endothermic by an amount Q , then the incoming neutron must have an energy greater than Q for the reaction to be energetically possible. Thus, the cross section for this particular reaction is zero for energies less than $\frac{(A+1)Q}{A}$, where A is the atomic weight of the target nucleus. As

explained below, it may be possible to use this reaction to measure the integrated energy-dependent flux above the threshold. In exothermic reaction, the threshold is determined by the coulomb barrier penetration of the interacting particles. An example of this is the fission cross-section threshold of heavy elements with an even atomic mass number, such as U234 and U238.

In this case, the coulomb barrier that must be overcome by the fission fragments is greater than the binding energy of the absorbed neutron, and so the incoming neutron must supply the energy difference.

All of the threshold reactions used for detection purposes today are of the (n,p), (n, α), (n,2n), or (n,f) type. The (n,2n) reaction is highly endothermic, having thresholds in the 5-to-10 Mev energy range, and above. The (n, α) reaction has a large coulomb barrier that produces thresholds of the order of 5 to 10 Mev. The (n,p) reaction is usually endothermic as well as hindered by the coulomb barrier, and thresholds greater than 1 Mev can be expected. The (n,f) reaction also has thresholds outside of the energy range of interest for even atomic mass number. For odd atomic mass numbers effective thresholds have been produced by using boron shielding, but these artificial thresholds are subject to error and still are not in the right part of the spectrum. In the search for threshold detectors in the Kev energy range, it was decided to ignore the types of reactions mentioned above because of their seeming inability to produce thresholds in the right range and because of the difficulty of obtaining cross-section data on these reactions.

The only common threshold reaction not mentioned above, and one that appears to have been ignored up to this time, is the (n,n') reaction, or inelastic scattering. In this process the neutron interacts with the nucleus and is scattered, but the nucleus is left in an excited state -- thus the term inelastic scattering. In most cases, the excited nucleus immediately returns to its ground state with the emission of a gamma ray. However, in certain nuclei the lifetime in an excited state may be of the order of minutes, hours, or even days. These long-lived excited states are known as isomeric states, and the excited nucleus is called an isomer of the ground-state nucleus. Thus we are provided with a simple means of telling how many inelastic scattering reactions to a given isomeric state have occurred--by measuring the decay rate of the isomeric state after irradiation by the neutron flux. It also turns out that the energy of these isomeric states is between 50 Kev and 2.2 Mev, thus providing thresholds in the region of interest.

A thorough search of the nuclide charts was made to choose the best possibilities for the threshold detectors. The choices were determined by four criteria: (1) proper location of threshold (10 through 600 Kev), (2) sufficient isomer half-life (> 0.5 sec), (3) low internal conversion of gamma rays and (4) freedom from competing reactions.

No consideration was given to the availability of the pure isotope or to magnitude of the cross section (only very limited cross-section data are available at present). Table 1A presents the best prospects for stable isotopes, and table 1B presents the best prospects for long-lived radioactive isotopes. The threshold was determined from the

relation $E_t = \frac{A+1}{A} QI$ where QI is the energy of the isomeric state and A is the atomic mass of the scattering nucleus in amu. The extra energy

TABLE IA--Stable Isotopes

Isotope	Isomer half-life	Threshold (Kev)	Internal conversion coefficient	Gamma energy (Kev)	Competing reactions & thresholds (Mev)
Ba ¹³⁷	2.6 ^m	667	$\frac{e}{\gamma} = .12$	662	(n,p) - 1.21
Hg ¹⁹⁹	4 ^m	523	$\frac{e}{\gamma_1} = 1.8, \frac{e}{\gamma_2} \sim .5$	$\gamma_1 = 33, \gamma_2 = 158$	(n,p) - ?
Cd ¹¹¹	48.6 ^m	339	$\frac{e}{\gamma_1} \sim 3, \frac{e}{\gamma_2} = .064$	$\gamma_1 = 148, \gamma_2 = 247$	(n,p) - 1.12
Sr ⁸⁷	3.8 ^h	333	$\frac{e}{\gamma} \sim .27$	338	None
Hf ¹⁷⁹	19 ^s	377	$\frac{e}{\gamma_1} \sim 33, \frac{e}{\gamma_2} = .05$	$\gamma_1 = 170, \gamma_2 = 215$	None
Sn ¹¹⁷	14 ^d	323	$\frac{e}{\gamma_1}$ large, $\frac{e}{\gamma_2} ?$, $\frac{e}{\gamma_3} = 0.1$	$\gamma_1 = 159, \gamma_2 = 330, \gamma_3 = 161$	(n,p) - 1.49
Ba ¹³⁵	9 ^h	270	$\frac{e}{\gamma} \sim 4$	463	None
Pt ¹⁹⁵	3.5 ^d	261	$\frac{e}{\gamma_1}$ large, $\frac{e}{\gamma_2} \sim 8, \frac{e}{\gamma_3} = 9$	$\gamma_1 = 130, \gamma_2 = 31, \gamma_3 = 39$	(n,p) - 2.14
Er ¹⁶⁷	2.5 ^s	209	$\frac{e}{\gamma} \sim 2$	308	(n,p) - ?
Te ¹²⁵	59 ^d	146	$\frac{e}{\gamma_1} \sim 300, \frac{e}{\gamma_2} \sim 15$	$\gamma_1 = 110, \gamma_2 = 35$	(n,p) - 0.745
Sn ¹¹⁹	150 ^d	89.8	$\frac{e}{\gamma_1} ?$, $\frac{e}{\gamma_2} \sim 7$	$\gamma_1 = 65, \gamma_2 = 24$	None

TABLE IB--Long-Lived Isotopes

Isotope	Isomer half-life	Threshold (Kev)	Internal conversion coefficient	Gamma energy (Kev)	Competing reactions & thresholds (Mev)
* ⁷⁹ Se	3.9 ^m	97.2	$\frac{e}{\gamma} \sim 12$	96	(n,p) - 2.30
** ¹²³ Te	104 ^d	250	$\frac{e}{\gamma_1}$ very large,	$\gamma_1 = 89,$	None
			$\frac{e}{\gamma_2} \sim 0.19$	$\gamma_2 = 159$	

* 6.5×10^4 y half-life

** $> 10^{14}$ y half-life

s--second, m--minute, h--hour, d--day, y--year.

is needed to conserve momentum in the process. The e/γ ratio is the number of internal conversion electrons emitted per gamma ray emitted by the decaying isomers. Since it is easier to eliminate competing radiations by gamma spectroscopy, the e/γ ratio should be as small as possible. When several gammas are given, the isomer can decay by several paths or in a cascade.

Of the isotopes in tables 1A and 1B, the only one for which suitable cross section data were available was Barium-137. To investigate the feasibility of this flux measurement system, it was decided to attempt flux measurements with the Ba^{137} in the General Atomic Triga reactor at Torrey Pines, California, and to compare the results with those from a standard threshold detector. The standard detector used in this test was Sulfur-32, which measures the integrated flux above 2.9 Mev by means of the $S^{32}(n,p)P^{32}$ reaction. Since the Ba^{137} measures the integrated flux above 1.9 Mev, a comparison of the plots of the sulfur and barium fluxes should give a good picture of the accuracy and consistency of the new method. This describes the testing procedure and gives the results and conclusions of the test that was performed 22 through 25 August 1960.

2. THEORY

The rate at which a specific neutron-induced reaction occurs in a reactor is given by

$$R = \int_V \int_0^{\infty} \Sigma(\vec{r}, E) \phi(\vec{r}, E, t) dV dE$$

where Σ is the macroscopic cross section for the reaction and ϕ is the energy-dependent neutron flux. If the volume considered is small enough Σ and ϕ may be considered constant in space and the formula reduces to

$$R = V \int_0^{\infty} \Sigma(E) \phi(E, t) dE. \quad \text{If the reaction considered has a threshold, that}$$

is, the cross section is zero below an energy E_t , then the formula becomes

$$R = V \int_{E_t}^{\infty} \Sigma(E) \phi(E, r) dE$$

Finally, if Σ is constant above E_t , which is a step function, then

$$R = \Sigma V \int_{E_t}^{\infty} \phi(E, t) dE = \Sigma V \phi_{int}^*(t) \quad \text{where } \phi_{int}^* \text{ is the energy-integrated}$$

neutron flux above E_t . If N_0 is the number of atoms of the product of the reaction present at time t , then

$$\frac{dN_0}{dt} = R - \lambda N_0 = \sum V \phi_{int}^*(t) - \lambda N_0$$

where λ is the decay constant of the product. The solution to this equation is $N_0(t) = e^{-\lambda t} \int_0^t e^{\lambda t'} \sum V \phi_{int}^*(t') dt'$. In a pulse reactor such as Triga, the pulse duration is of the order of milliseconds, and $\lambda t' \ll 1$ for half-lives greater than 0.1 sec. In this case

$$N_0 = \int_0^t \sum V \phi_{int}^*(t') dt' = \sum V \phi_{int} \text{ immediately after the pulse, where}$$

ϕ_{int} is the time and energy integrated neutron flux above E_t . After removal from the flux, the product of the reaction will decay with its characteristic decay constant λ , if it is unstable. The number of product atoms remaining at a time t sec. after removal from the flux is $N = N_0 e^{-\lambda t}$, and the decay rate is $A = \lambda N = \lambda N_0 e^{-\lambda t}$. Thus, by measuring the decay rate and knowing λ , N_0 can be determined. From this, ϕ_{int} can be calculated if \sum and V are known.

Barium-137 has an isomeric excited state producing a 660 Kev gamma ray with a half-life of 2.60 min. The cross section for inelastic scattering to this state is shown in figure 1. This cross section includes direct excitation to the isomeric level and excitation to higher levels that immediately decay to the isomeric level. The higher-level excitation gives rise to the several jumps in the cross-section curve. The ideal case would be where only direct excitation is possible. Then the cross-section curve would more nearly resemble a step function. Since the values of the cross section have only been measured up to 3 Mev, it will have to be assumed that the cross section levels off and remains constant at 600 millibarns. Future measurements will have to be extended to at least 10 Mev to make accurate calculations. The actual cross section will have to be replaced by a step function with an effective threshold in order to use the threshold technique described earlier. The effective threshold is determined from the relation

$$\text{step} \int_{E_{eff}}^{\infty} \phi(E) dE = \int_{E_t}^{\infty} \sigma(E) \phi(E) dE$$

where $\phi(E)$ is the flux into which the barium is to be placed. Although $\phi(E)$ is not known, it is assumed to be close to a fission spectrum, and

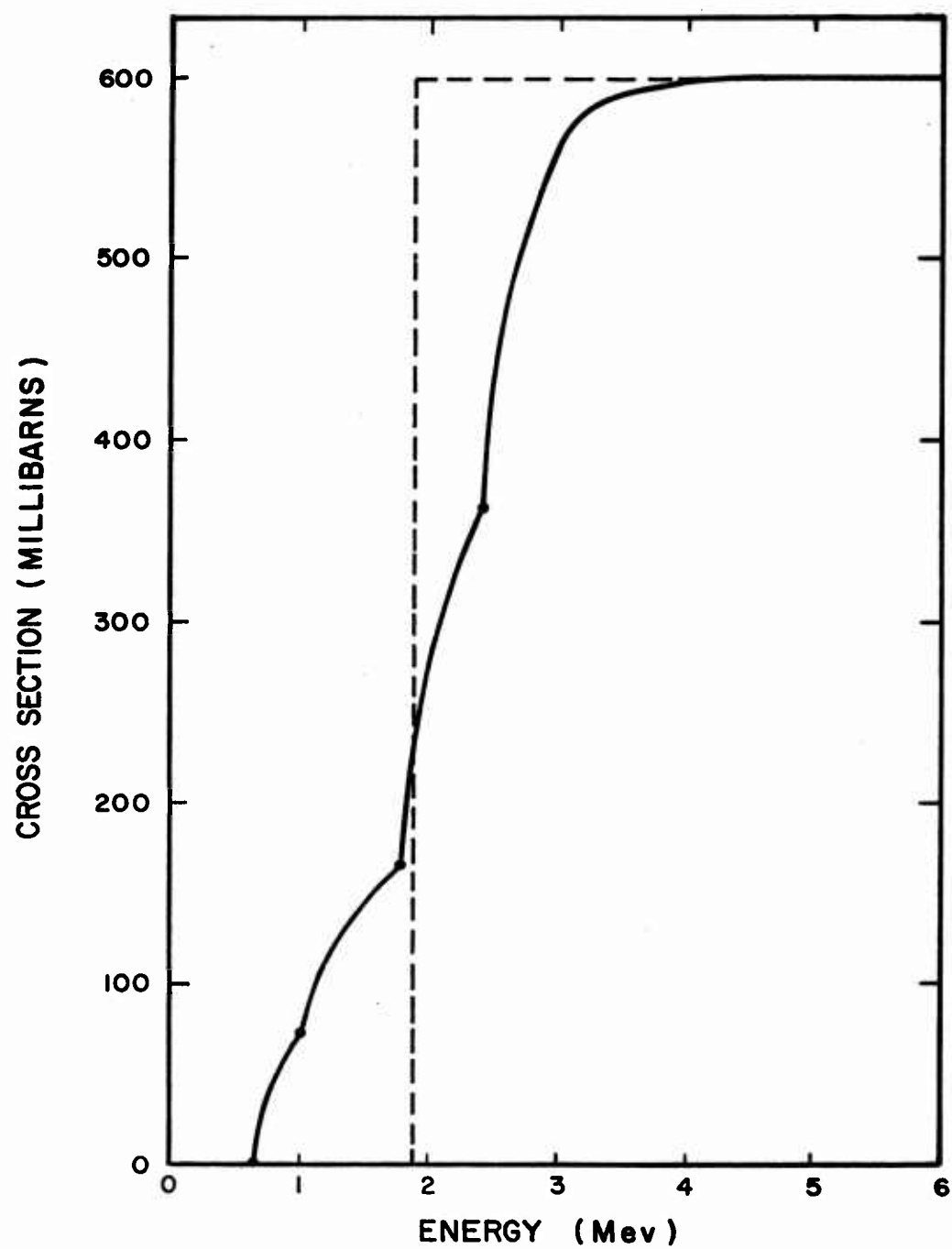


Figure 1. Real and effective cross sections for the reaction $\text{Ba}^{137}(n,n')\text{Ba}^{137m}$ versus energy

it has been shown that E_{eff} is not very sensitive to changes in the shape of $\phi(E)$. Thus a fission spectrum can be assumed for $\phi(E)$, and the above equation can be numerically integrated to give E_{eff} . In the present case $E_{eff} = 1.9$ Mev if the height of the step is 600 millibarns. Once a flux spectrum has been determined by the use of many foils, this known spectrum can be used to get new E_{eff} 's. This iterative process can be repeated until the E_{eff} 's stabilize. In actual practice, it will probably turn out that the original E_{eff} 's do not change appreciably when the new spectrum is used. The step cross section is also shown in figure 1.

3. EQUIPMENT

Since costs prohibited obtaining pure Ba^{137} , the detectors were made of natural $BaCO_3$ powder inclosed in watertight plastic capsules. The capsules were made by drawing hot polyethylene over a brass form by air suction (figure 2). The capsules were then packed with a known weight of powder (approximately 1 gram) and heat sealed (figure 3).

To eliminate as many competing reactions as possible, it was necessary to shield the pellets from thermal neutrons to prevent various (n,γ) reactions from occurring. This was done by placing the capsules inside a cadmium shield approximately 30 mils thick. This decreased the thermal flux at the pellet by a factor of 10^4 , while letting over 99 percent of the fast neutrons through. The only other reaction that produces appreciable radiation besides the various (n,γ) ones is the (n,n') reaction in Ba^{135} . However, this produces a 268-keV gamma ray that does not interfere with the 660-KeV gamma of Ba^{137m} .

Gamma ray counting was done with a $NaI(Tl)$ crystal, Dumont 6292 photomultiplier tube, Hamner N351 preamplifier, Hamner N401 high-voltage power supply, Hamner N302 pulse-height analyzer, and a Hupp model 400 counter.

4. PROCEDURE

Flux measurements were made on the General Atomic Triga reactor. Triga is a water and zirconium hydride-moderated, water-cooled, pulse-type reactor with a cylindrical core. Surrounding the cylindrical core is a graphite reflector. All measurements were made outside the core of the reactor. A core diagram, showing positions of fuel elements and control rods in the top grid plate, is shown in figure 4. In each measurement a cadmium-covered barium pellet and a sulfur pellet were used together. Positioning of the pellets was accomplished by lowering them through 16 ft of water with a string. Four traverses were made across the face of the top grid plate as shown in figure 4. Traverses I, II, and III were each made twice, while traverse IV was only made once. Several circular traverses were made on the top grid plate over the F-ring, and one vertical traverse was made from the top grid plate to 20 in. above the plate.



Figure 2. Brass form for producing plastic capsules

2162-60

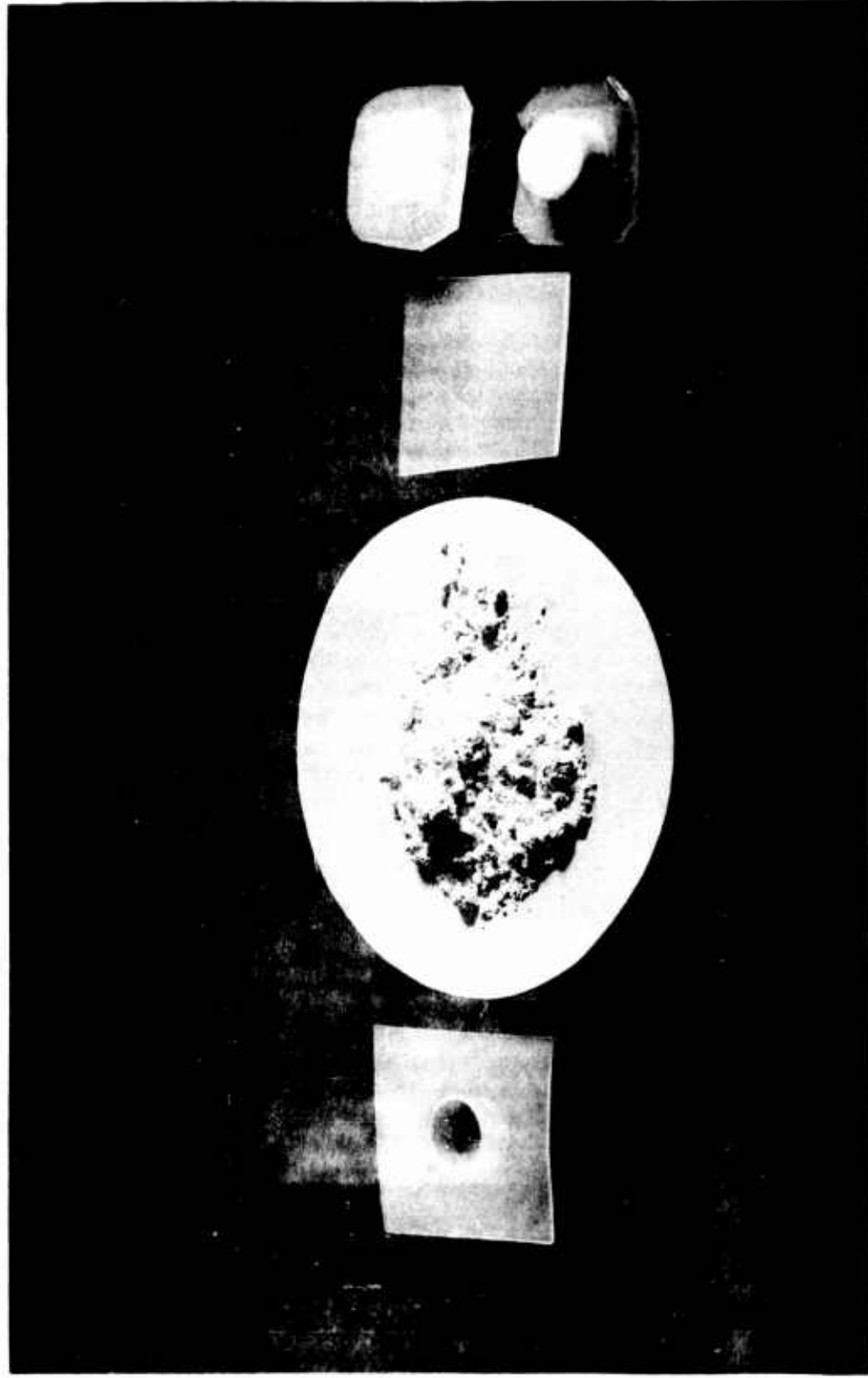


Figure 3. Method of increasing BaCO₃ powder in plastic capsule

2164-60

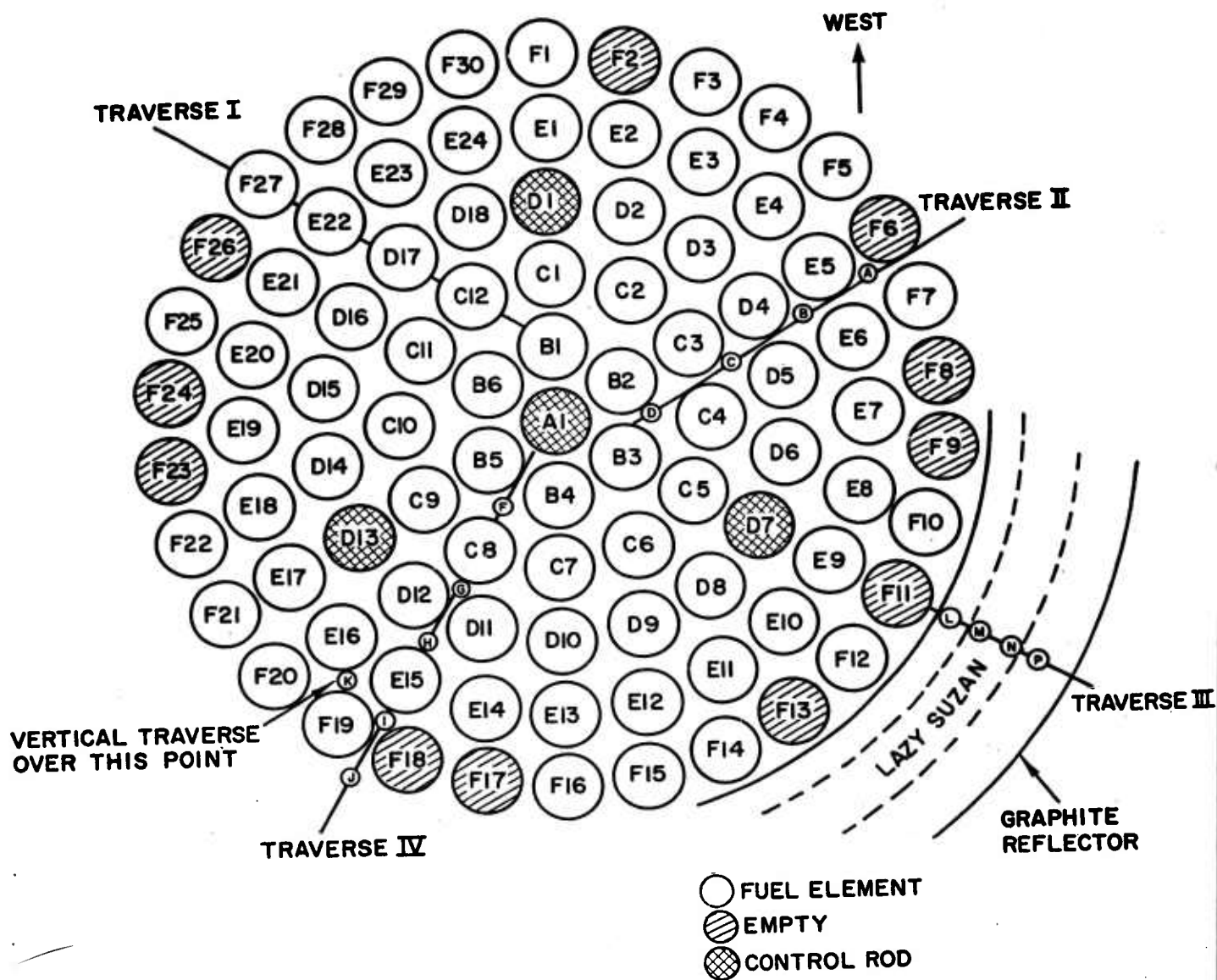


Figure 2. Diagram of top grid plate

After the barium pellets were irradiated they were immediately removed from the reactor, taken out of their cadmium shields, and counted. Three counts of 30-sec duration for each pellet were made several minutes apart. Thirty or more minutes after irradiation, the pellets were again counted to determine the long-lived background activity. This was subtracted from the original counts to get the actual $\text{Ba}^{137\text{m}}$ activity. Only counts in the photopeak for the 660-Kev gamma ray were recorded. This cut down considerably the residual background. The efficiency of the counting system was determined periodically by means of a calibrated Cl^{137} source, which decays to $\text{Ba}^{137\text{m}}$, and thus emits the same gamma ray. This efficiency measurement included geometry, scattering, and gamma-ray internal conversion factors, but did not include self-shielding factors, which were assumed negligible for the small pellets. Only five pellets could be irradiated at any one time because the short half of the $\text{Ba}^{137\text{m}}$ limited the time available for counting. The sulfur pellets were shipped to the Army Chemical Center at Edgewood, Maryland, for counting and flux evaluation.

5. REDUCTION AND ANALYSIS OF DATA

Table 2 shows the steps by which the raw data were reduced to give the barium flux ($\phi_{1.9}$). The residual background was subtracted from the measured counting rates to give the numbers in the C-B column. This column gives the number of counts recorded by the pulse height analyzer that came only from the decay of $\text{Ba}^{137\text{m}}$. A plot of C-B versus time after irradiation on semilog paper will give a straight line whose slope is equal to the decay constant of the $\text{Ba}^{137\text{m}}$ (i.e., 0.266 min^{-1}). Figure 5 shows these plots for the four pellets in table 2. The zero time intercept of this graph gives the number of counts that would be recorded in 30 sec immediately after irradiation. These numbers are given in the graph intercept column. The next column, A'_0 , is simply the graph intercept column converted to counts per minute. The conversion factor is 2.13 instead of 2 in order to correct for the decay of the $\text{Ba}^{137\text{m}}$ during counting. The efficiency of the system was determined by use of a calibrated Cs^{137} source as mentioned previously. A_0 is the actual decay rate of the $\text{Ba}^{137\text{m}}$ at zero time and is simply given by $A_0 = \frac{A'_0}{(\text{efficiency})}$. It was shown above that $N_0 = \sum \text{step } V \phi_{1.9}$. We also have $\sum \text{step} = \frac{N \sigma}{V}$ step where N = number of Ba^{137} atoms in volume V . Thus, $\phi_{1.9} = \frac{N_0}{N \sigma \text{ step}} = \frac{A_0}{N \sigma \text{ step}}$. N is given by

$$N = \frac{W (6.02 \times 10^{23}) \alpha}{(\text{MW})}$$

where W = pellet weight

MW = molecular weight of BaCO_3

α = percent abundance of Ba^{137}

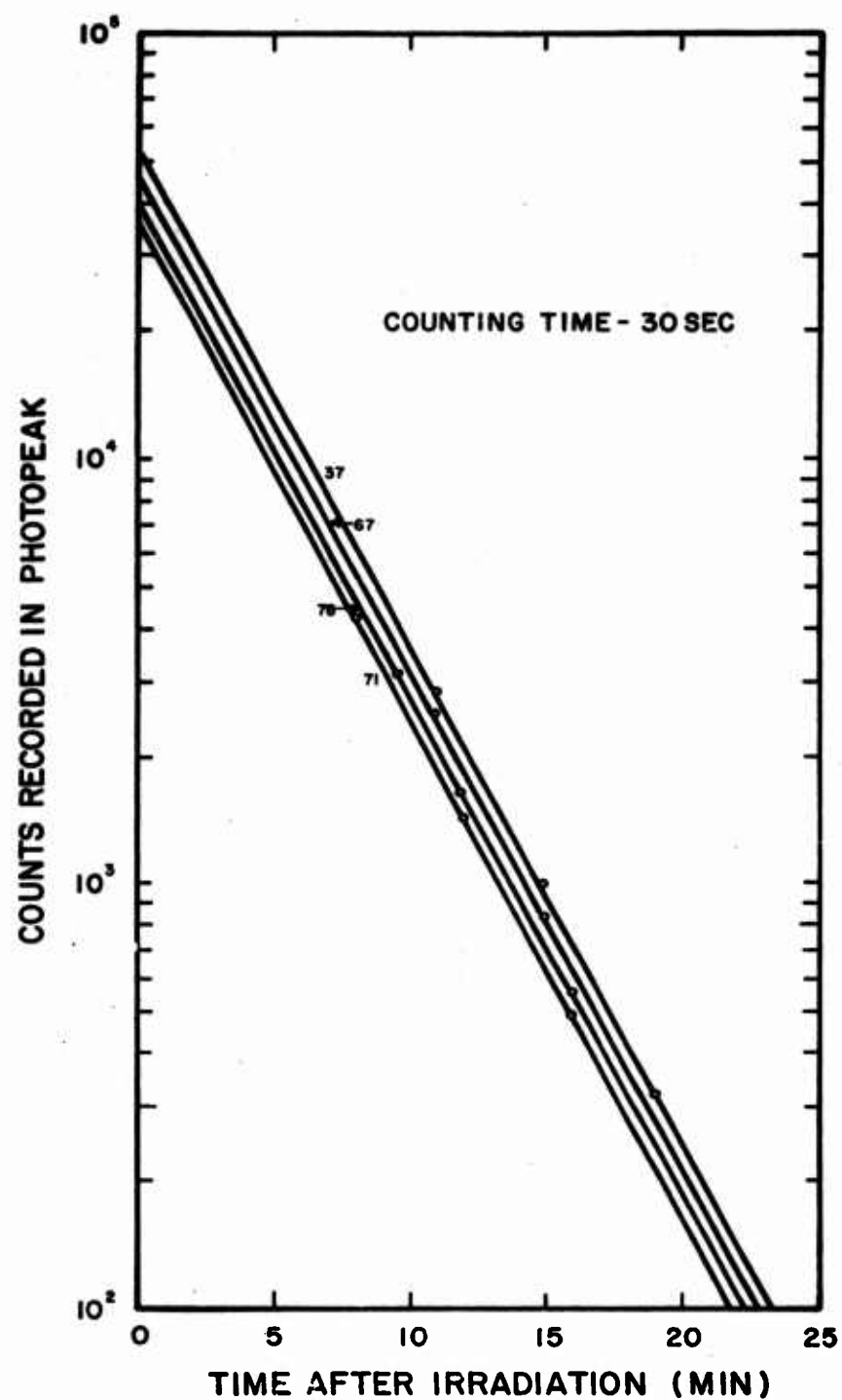


Figure 5. Decay curves for barium pellets in table 2
(C-B versus time after irradiation)

TABLE 2. Examples of data reduction for several pellets

Barium (pellet number)	Time after irradiation (min)	Counting time (sec)	Number of counts (C)	Residual background (B)	$\frac{(C-B)}{2}$	Graph C-B intercept	$\frac{(C-B)}{2}$	Corrected A_0	Counter efficiency	A_0 (cpm)	Pellet weight (grams)	Barium flux $\phi_{1.9}$	Sulfur flux $\phi_{2.9}$ (n/cm ²)
37	11	30	28,700		27,900								
	15	30	10,700		9,900		5.30×10^5	11.3×10^5	.0071	15.9×10^7	0.98	2.92×10^{12}	1.51×10^{12}
	19	30	3,900		3,100								
	53	30											
67	7	30	65,000		64,400								
	11	30	25,700		25,100		4.65×10^5	9.90×10^5	.0071	13.9×10^7	1.08	2.32×10^{12}	1.17×10^{12}
	15	30	9,000		8,400								
	42	30											
71	8	30	42,800		42,100								
	12	30	14,600		14,100		3.60×10^5	7.67×10^5	.0071	10.8×10^7	1.16	1.68×10^{12}	$.89 \times 10^{12}$
	16	30	5,400		4,900								
	53	30											
78	9.5	30	31,400		30,700								
	12	30	17,200		16,500		4.10×10^5	8.73×10^5	.0071	12.3×10^7	1.08	2.05×10^{12}	1.40×10^{12}
	14	30	10,200		9,500								
	16	30	6,200		5,500								
	45	30											
					707								

$$N = \frac{W (6.02 \times 10^{23}) (.1132)}{(197.3)} = 3.45 W 10^{20}$$

and

$$\phi_{1.9} = \frac{A_o}{W} \times \frac{1}{(.2665)(3.45)(.6 \times 10^{-24}) \times 10^{20}}$$

$$\phi_{1.9} = 1.81 \frac{A_o}{W} \times 10^4$$

The sulfur and barium fluxes are given in the last two columns.

The best way to show the accuracy and consistency of this method is by a comparison of the graphs of sulfur and barium fluxes along various traverses in the reactor. Figure 6 shows the average of two runs made over traverse I. Figure 7 shows the average of two runs made over traverse II. Figure 8 shows the average of two runs made over traverse III. Figure 9 shows the results of a single run made over traverse IV. The single vertical traverse is shown in figure 10. The average of the circular F-ring traverses is presented in figure 11.

Figures 12, 13, and 14 show the need for cadmium shielding of the barium pellets. Figure 12 gives a spectrum analysis of the radiation emitted by a cadmium-covered barium pellet at various times after irradiation, made with the 256-channel spectrum analyzer at General Atomic. Figure 13 shows the same spectrum analysis for a pellet that was irradiated bare. It is easily seen that the presence of competing radiation almost obliterated the 660 Kev photopeak. Figure 14 shows the decay curves of bare and cadmium-covered pellets after long-lived residual background was subtracted. The curvature of the bare pellet data is caused by competing radiation with half-lives on the same order as that of the Ba^{137m} . This makes it very hard, if not impossible, to get an accurate value of A_o . Also an estimate of the contribution to A_o of the (n,γ) reaction in Ba^{136} is needed. From this it is seen that cadmium covers are a necessity.

If a fission spectrum is assumed in the energy regions of the sulfur and barium fluxes, the ratio $\frac{\phi_{Ba}}{\phi_S} = \frac{\phi_{1.9}}{\phi_{2.9}}$ can be calculated by numerical integration. This ratio comes out to be 1.88. Measured values of this ratio for sulfur-barium pellet pairs were in general between 2.2 and 1.6. The average value for all pellets used was 1.89.

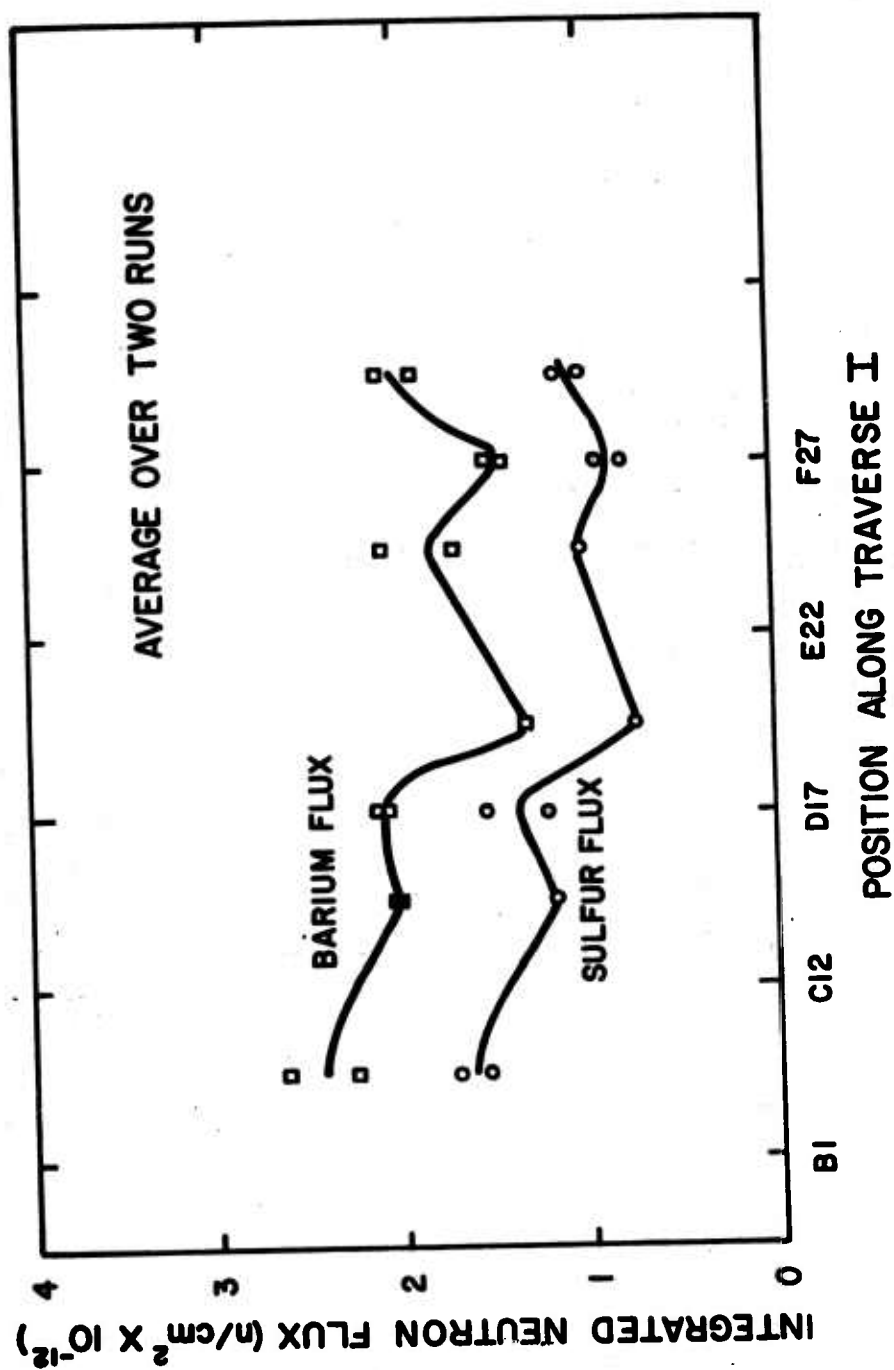
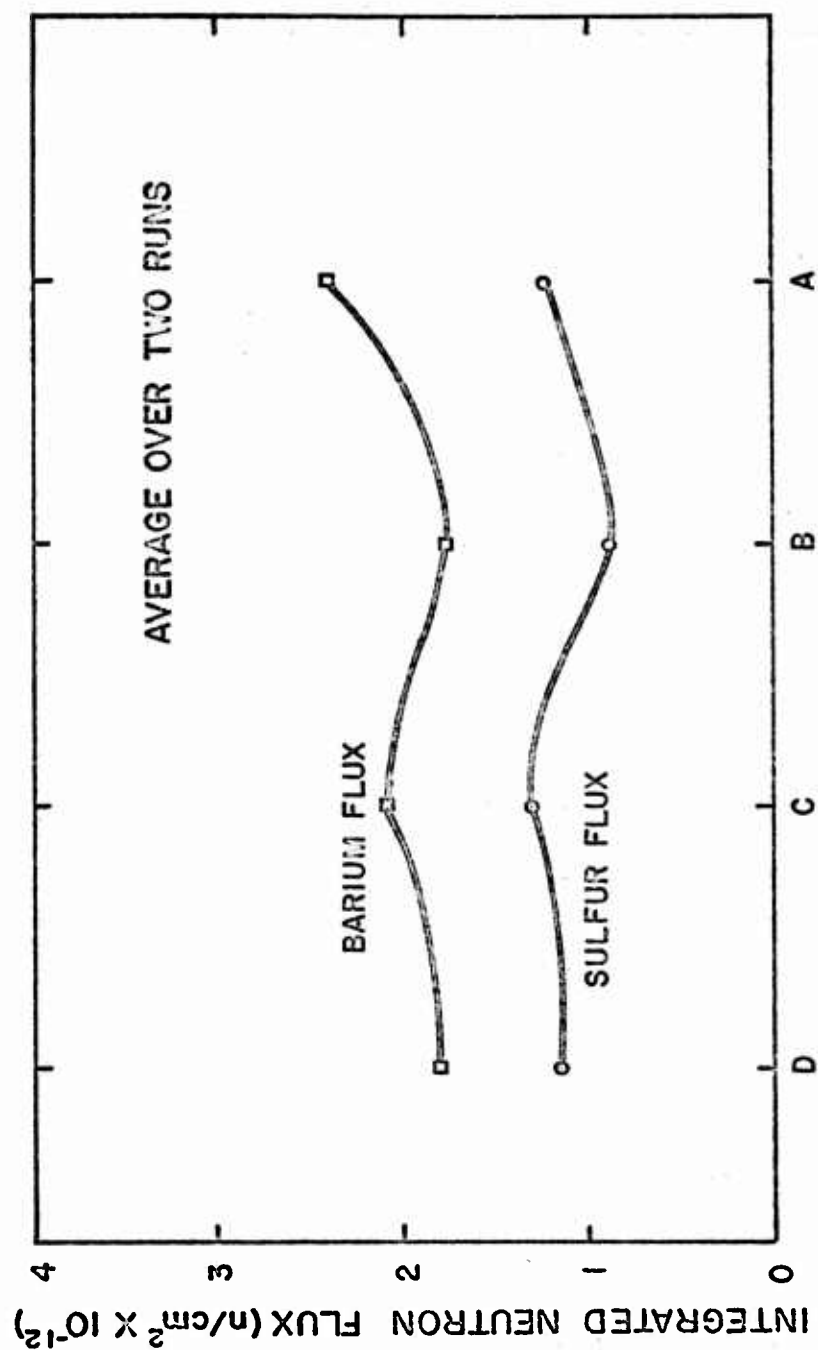


Figure 6. Integrated neutron flux along traverse I across top grid plate



POSITION ALONG TRAVERSE II

Figure 7. Integrated neutron flux along traverse II across top grid plate

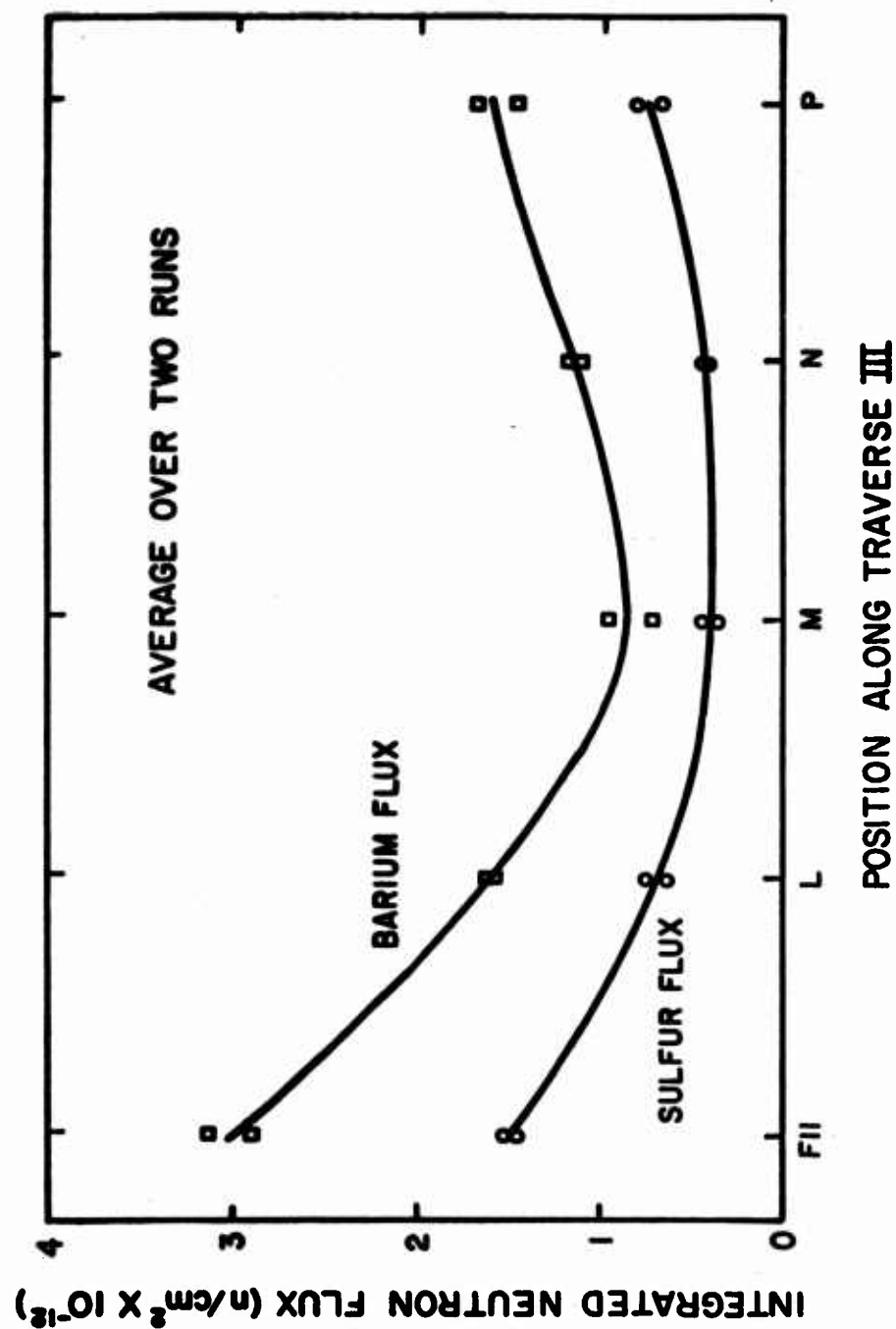


Figure 8. Integrated neutron flux along traverse III

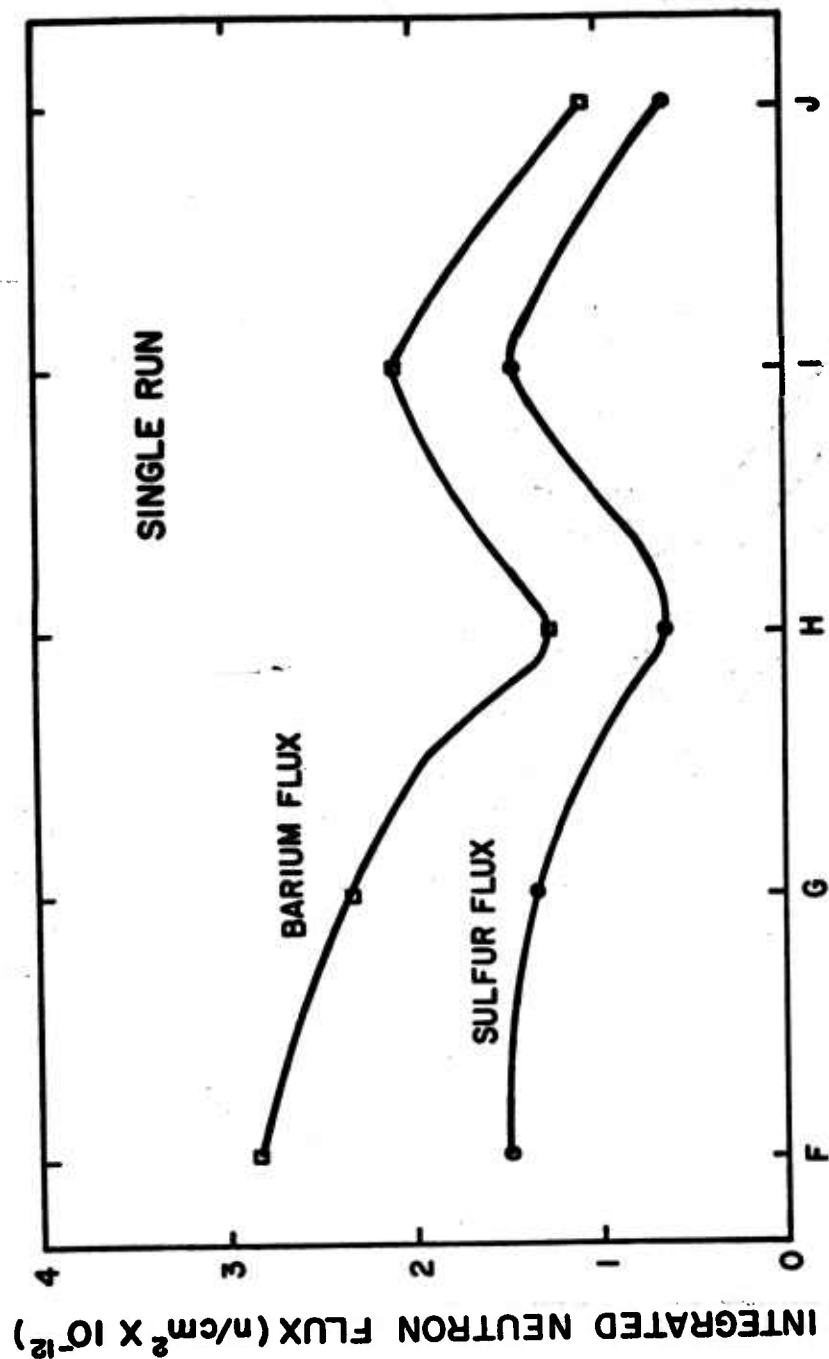


Figure 9. Integrated neutron flux along traverse IV across top grid plate

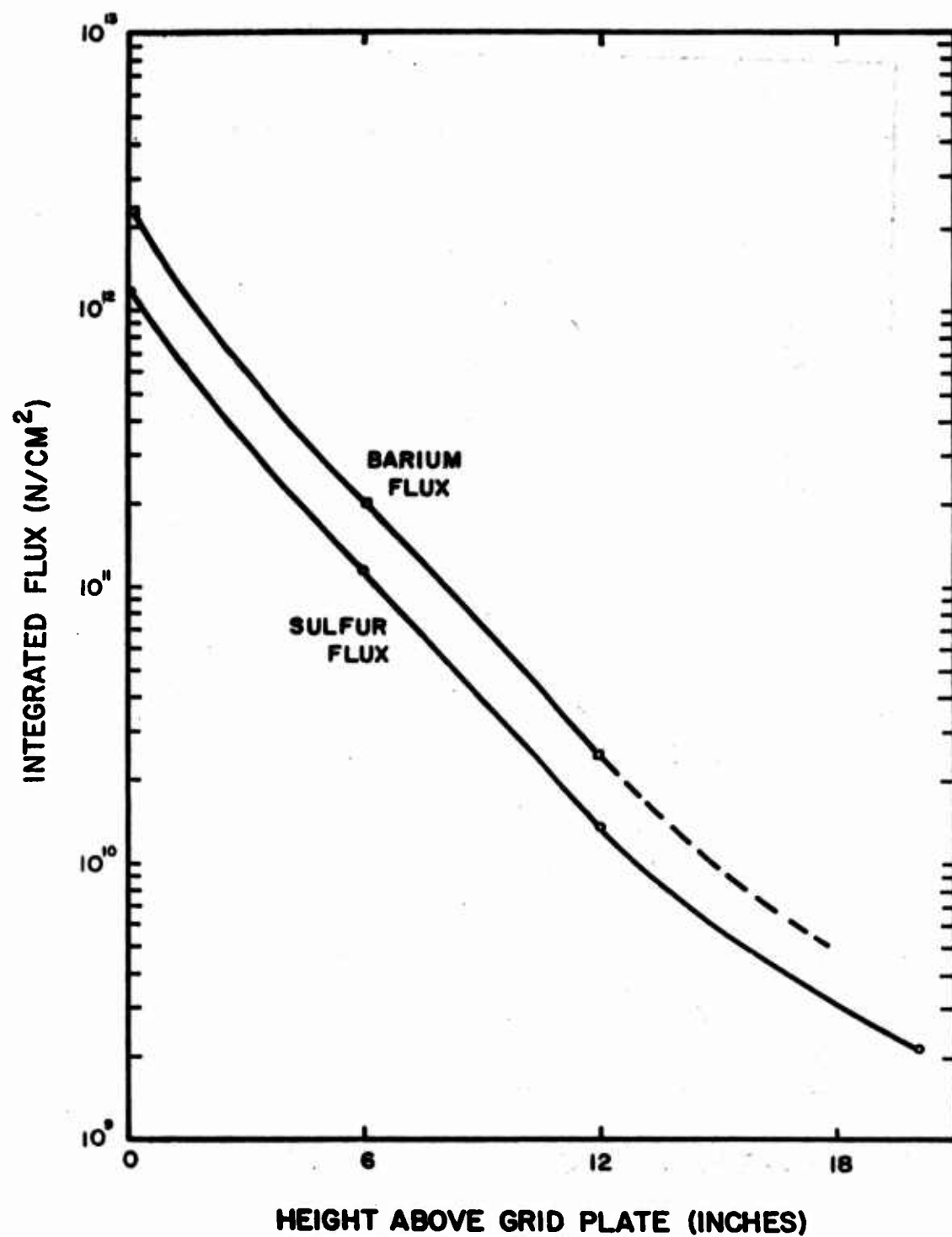


Figure 10. Integrated neutron flux versus height above position K on top grid plate

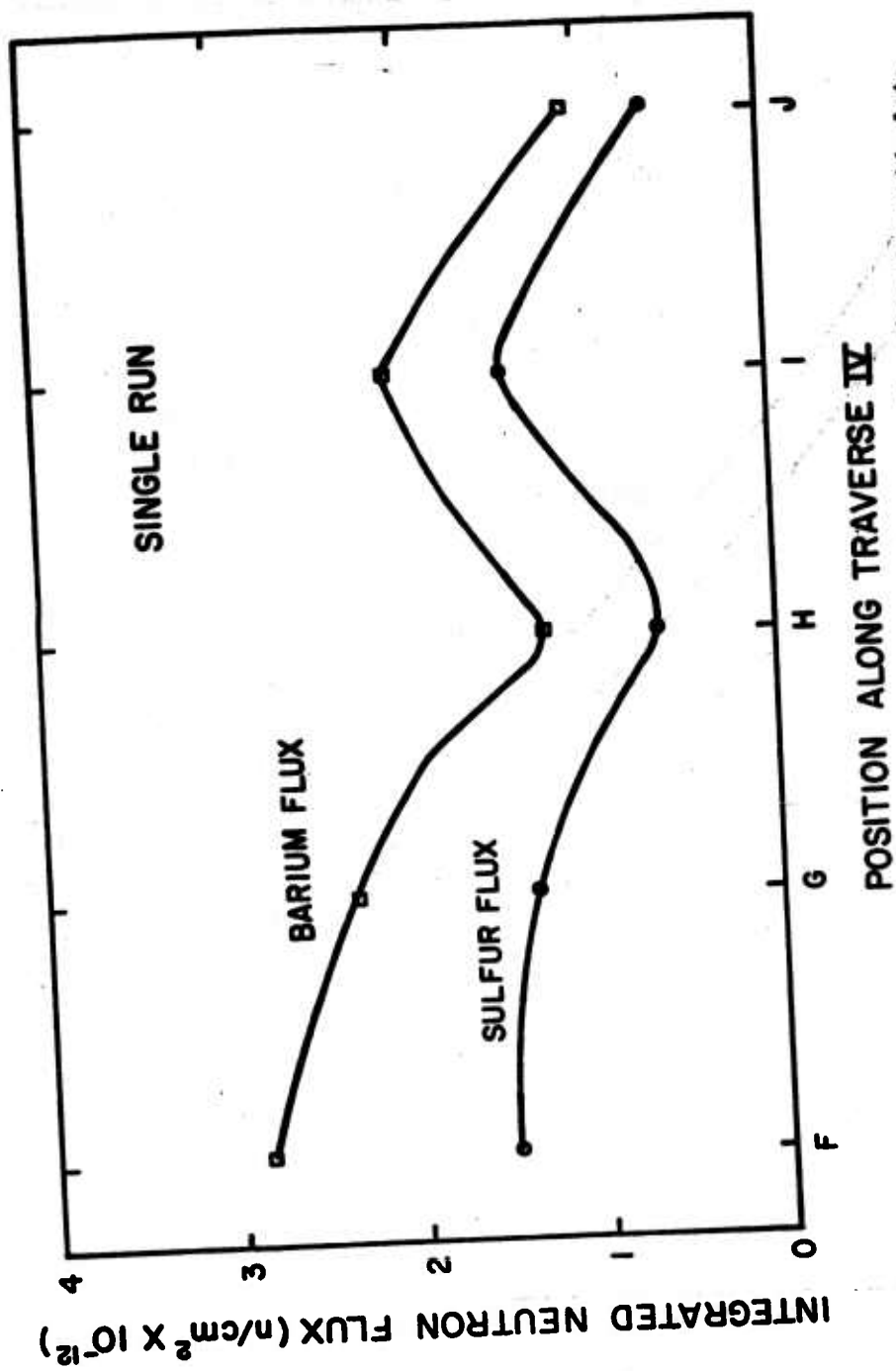


Figure 9. Integrated neutron flux along traverse IV across top grid plate

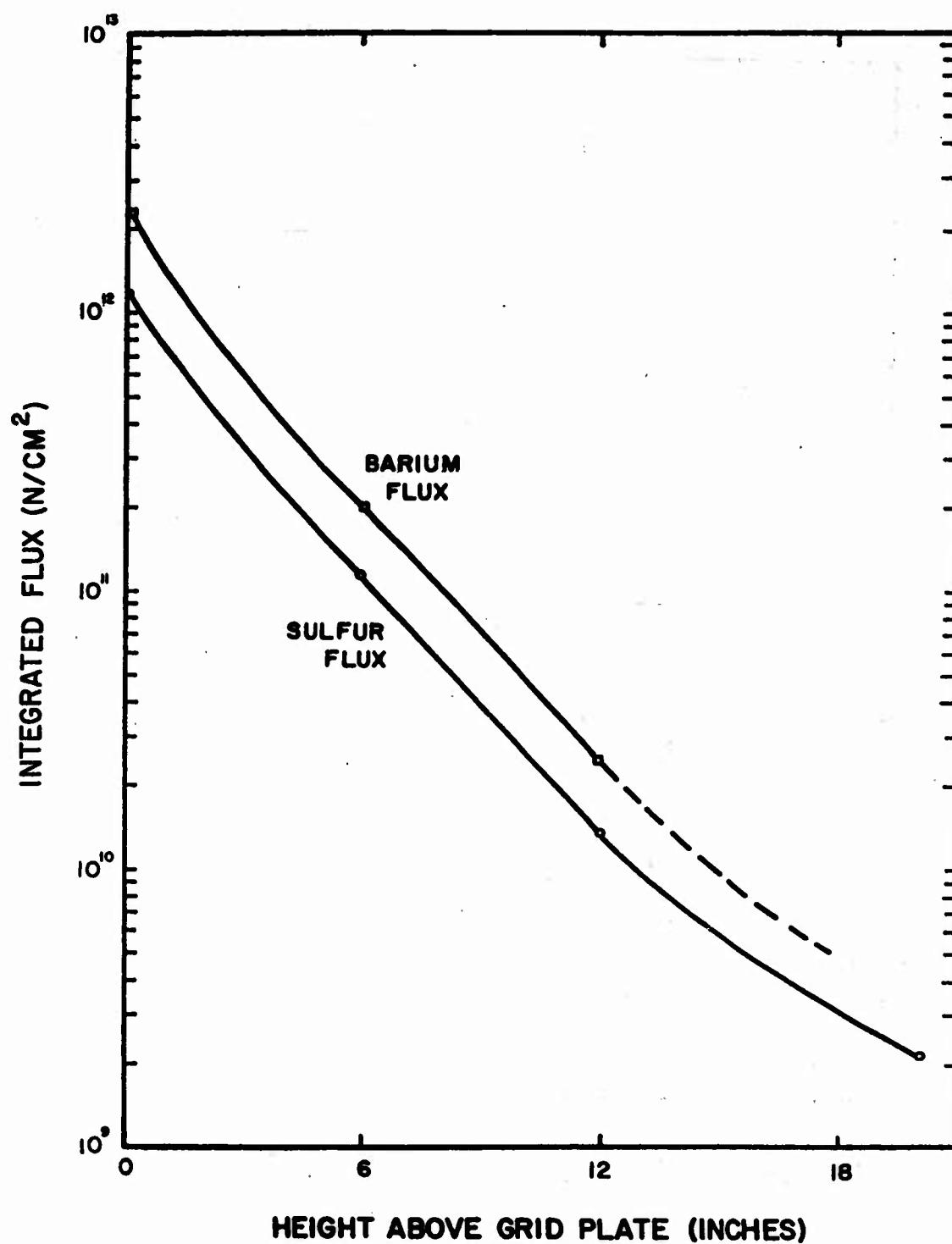


Figure 10. Integrated neutron flux versus height above position K on top grid plate

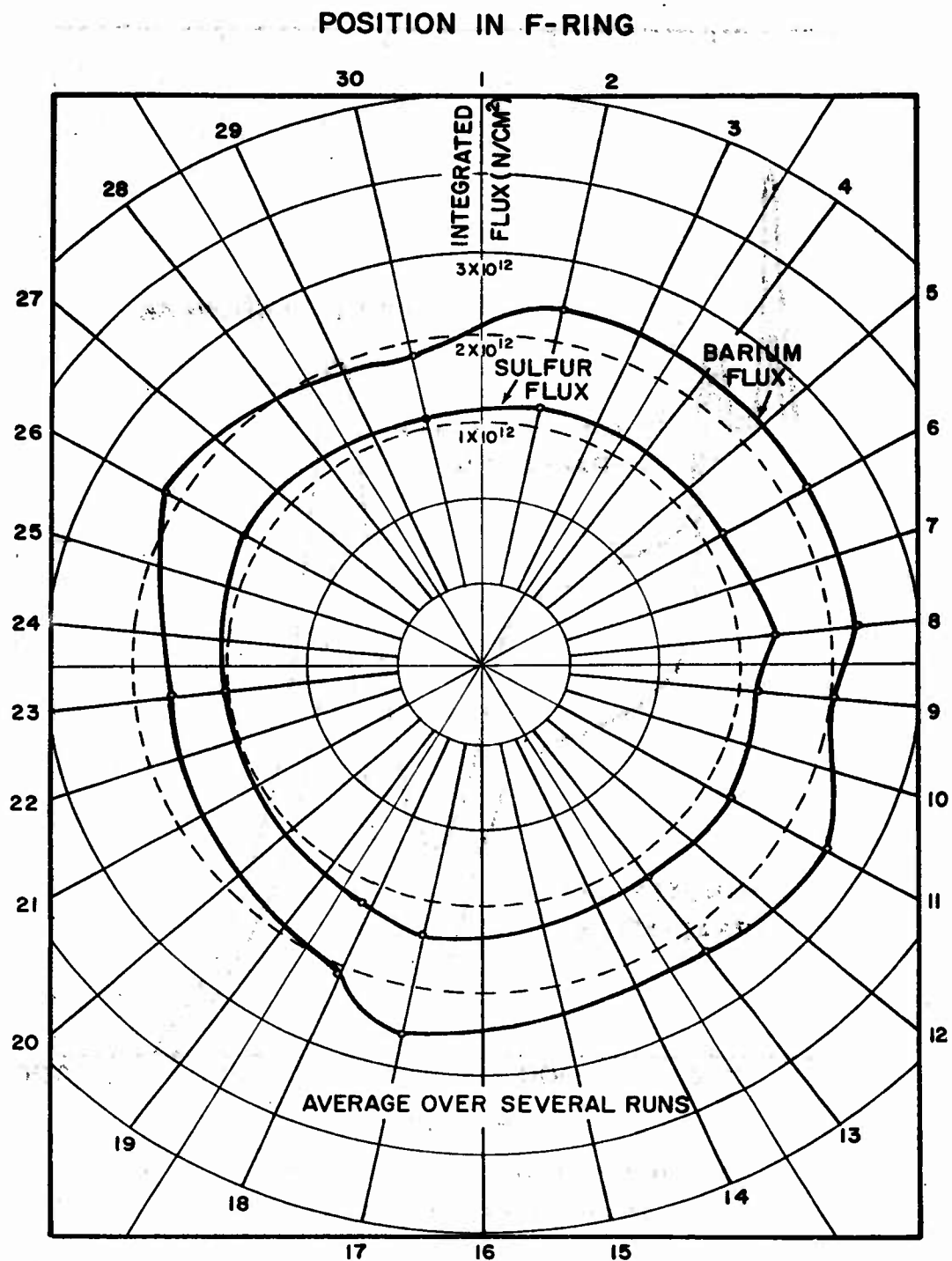


Figure 11. Average integrated neutron flux on top grid plate in F-ring

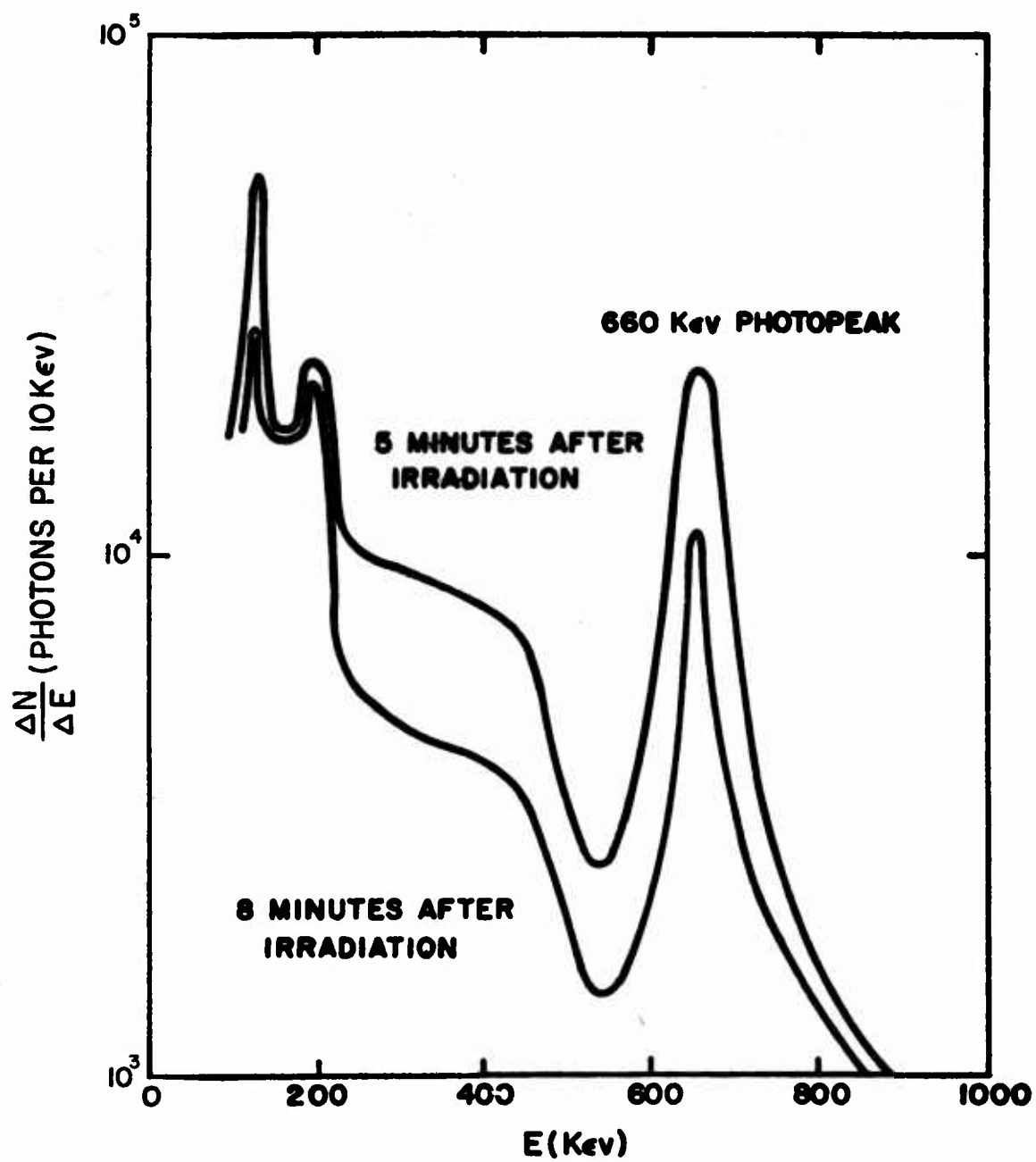


Figure 12. Differential gamma energy spectrum of BaCO_3 pellet irradiated in cadmium cover

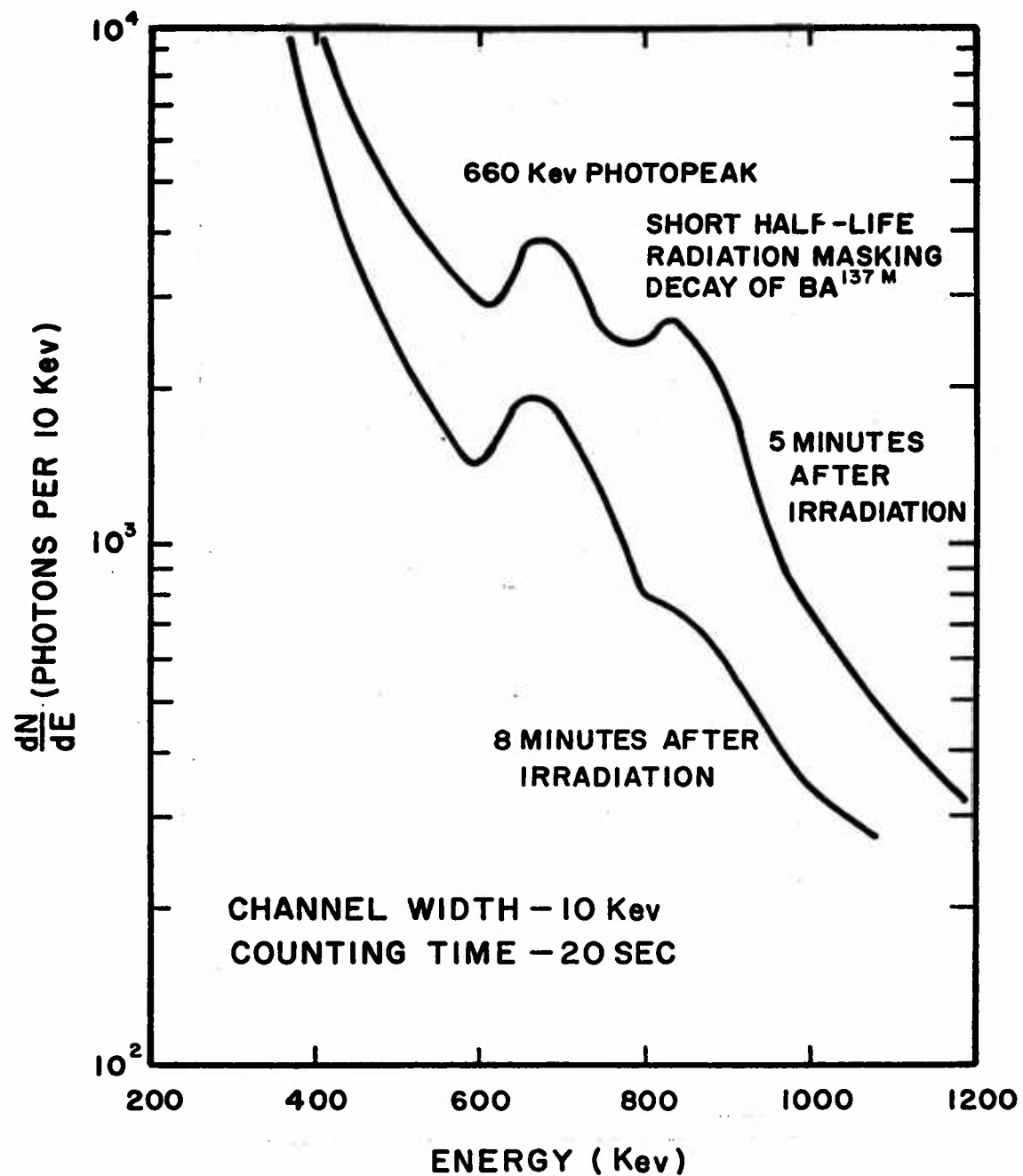


Figure 13. Differential gamma ray spectrum of BaCO_3 after bare irradiation by a neutron flux

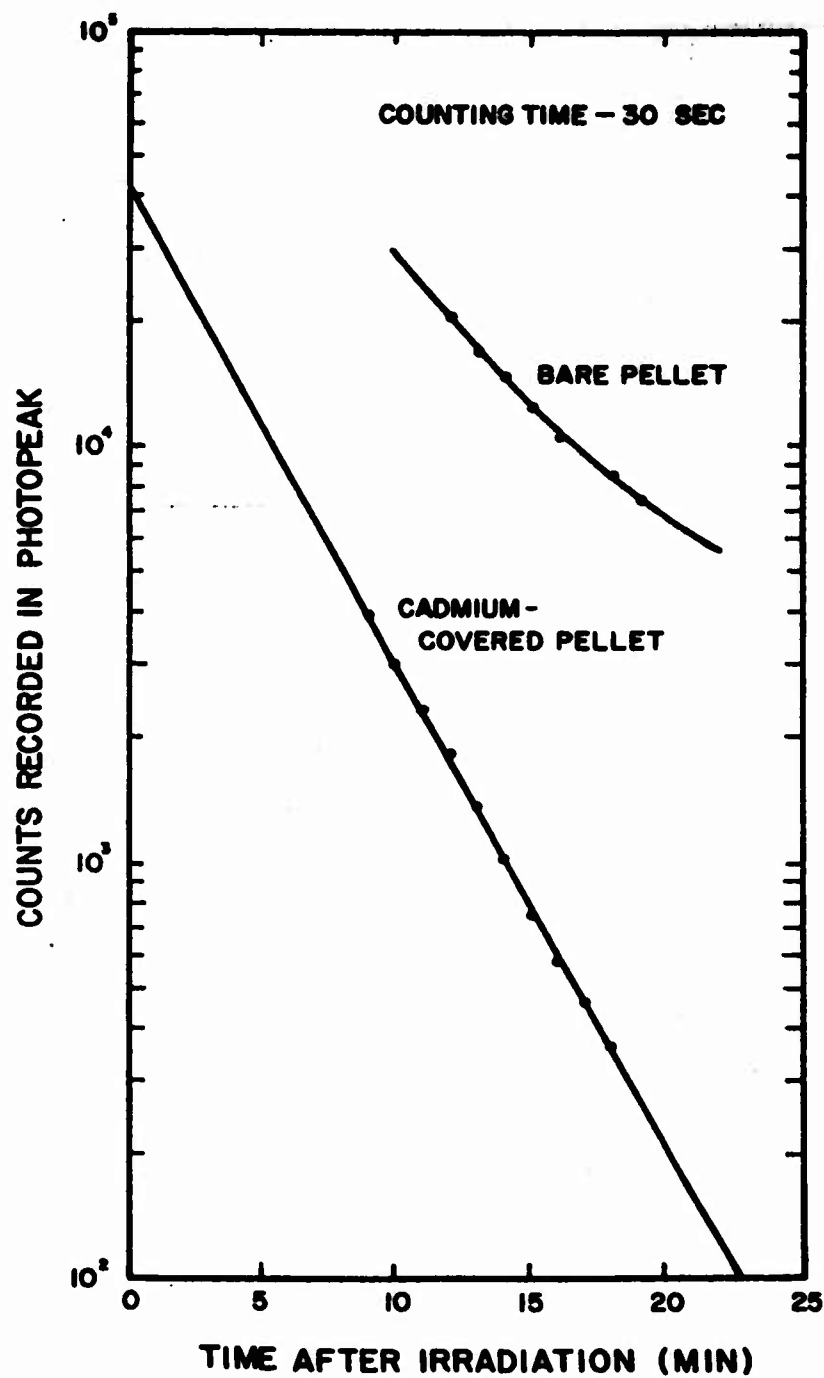


Figure 11. Comparison of decay curves of cadmium-covered and bare lanthanum pellets

6. CONCLUSIONS

The close correlation between the barium and sulfur flux plots and the agreement of the bariums to sulfur flux ratio with that predicted by the fission spectrum indicate that this foil detection system is at least as accurate and consistent as the systems now in use. Further, the ease in preparation and handling of the barium pellets is much greater than for other detectors now in use. Approximately 100 barium pellets were prepared in a single day at a material cost of less than one dollar. The counting procedure was also extremely simple and accurate as shown by the decay curves. All evidence indicates that a complete investigation of all nuclei with isomeric states as possible neutron detectors is desirable, and that it is likely that several new threshold detectors should result.

7. BIBLIOGRAPHY

Etherington, Harold, Nuclear Engineering Handbook, McGraw Hill Book Company, Inc., 1958.

Strominger, Hollander and Seaborg, Reviews of Modern Physics 30, 585 (1958).

Swann and Metzger, Physical Review 100, 1329 (1955).

Uthe, Paul M., Attainment of Neutron Flux Spectra from Foil Activations, Master's Thesis, Air Force Institute of Technology (1957).

DISTRIBUTION

Office of the Director of Defense Research & Engineering
The Pentagon, Washington 25, D. C.

Attn: Director of Electronics
Attn: Director of Weapons Systems Evaluation, Group (rm 2E812)
Attn: Ass't Director of Research & Engineering (Air Defense)
Attn: Technical Library (rm 3E1065) - 2 copies

Department of the Army
Office of the Chief of Ordnance
The Pentagon, Washington 25, D. C.
Attn: ORDTN (Nuclear & Special Components Br)
Attn: ORDTU (GM Systems Br)
Attn: ORDTB (Research Br)

Director, Army Research Office
Office of the Chief of Research & Development
Department of the Army
Washington 25, D. C.

Director, Special Weapons
Office of the Chief of Research & Development
Department of the Army
Washington 25, D. C.

Commanding General
Frankford Arsenal
Philadelphia 37, Pennsylvania
Attn: Dr. G. White
Attn: Reference Librarian

Commanding General
U.S. Army Ordnance Missile Command
Redstone Arsenal, Alabama
Attn: ORDXM-R (Ass't Chief of Staff for R & D)
Attn: Dr. W. Carter, Chief Scientist

Commanding General
Aberdeen Proving Ground, Maryland
Attn: BRL--Terminal Ballistics Laboratory, E. Minor
Attn: BRL--Weapons Systems Laboratory, F. E. Grubbs
Attn: Tech Library, Br No. 3, Bldg 400, D&P Services

Commanding General
Army Rocket & Guided Missile Agency
Redstone Arsenal, Alabama
Attn: ORDXR-R, Hugh Camp (R & D Div)
Attn: ORDXR-RHM (Antimissile Missile Br)

Commanding General
Army Ballistic Missile Agency
Redstone Arsenal, Alabama
Attn: Technical Documents Library

DISTRIBUTION (Continued)

Commanding Officer
Picatinny Arsenal
Dover, New Jersey
Attn: Mr. M. Weinstein
Attn: Library
Attn: Atomic Applications Library
Special Weapons Development Division

Commanding Officer
Chemical Warfare Laboratories
Army Chemical Center, Maryland
Attn: Librarian, Tech Library (Bldg 330)

Commanding Officer
U.S. Army Signal Research & Development Laboratory
Fort Monmouth, New Jersey
Attn: Electronic Components Research Dept
Attn: Library
Attn: SIGRA/SL-P, Lt E. T. Hunter

Commanding Officer
Ordnance Materials Research Office
Watertown Arsenal
Watertown 72, Mass
Attn: Dr. L. Foster

Commanding Officer
U.S. Army, Office of Ordnance Research
Box CM, Duke Station
Durham, North Carolina

Commanding General
OTAC
Detroit Arsenal
Centerline, Michigan
Attn: Mr. C. Salter

Commanding General
White Sands Missile Range, New Mexico
Attn: ORDDW-BS-OM, G. Elder

Commanding General
Ordnance Special Weapons-Ammunition Command
Dover, New Jersey

U.S. Continental Army Command
Liaison Group
The Pentagon (Rm 3E366)
Washington 25, D. C.

DISTRIBUTION (Continued)

Commandant
U.S. Army Artillery & Guided Missiles School
Fort Sill, Oklahoma
Attn: Combat Development Dept

Commandant
Command & General Staff College
Fort Leavenworth, Kansas
Attn: Archives

The Surgeon General
U.S. Army
Washington 25, D. C.
Attn: Special Ass't for Nuclear Energy
Attn: Research & Development Div

Department of the Navy
Washington 25, D. C.
Attn: Chief, Office of Naval Research (Bldg T-3)

Commander
U.S. Naval Ordnance Laboratory
Corona, California
Attn: Documents Librarian

Commander
U.S. Naval Ordnance Laboratory
White Oak, Silver Spring 19, Maryland
Attn: Tech Library

Department of the Navy
Bureau of Naval Weapons
Washington 25, D. C.
Attn: DLI-3, Tech Library

Commander
Naval Research Laboratory
Washington 25, D. C.
Attn: Tech Library

Department of the Air Force
Deputy Chief of Staff for Development
The Pentagon, Washington 25, D. C.
Attn: Director of Research & Development

Commander
Air Research & Development Command
Andrews Air Force Base
Washington 25, D. C.

DISTRIBUTION (Continued)

**Air Force Cambridge Research Center
Bedford, Mass.
Attn: R. Roberts**

**Commander
Air Force Special Weapons Center
Kirtland Air Force Base, New Mexico
Attn: Code SWVSE, L. Stewart
Attn: Lt. Col. F. Grose**

**Commander
Wright Air Development Division
Wright-Patterson Air Force Base, Ohio
Attn: Lt. Col. V. Bryson**

**Commander
Air Force Ballistic Missile Div (ARDC)
P. O. Box 262
Inglewood, California
Attn: WDSOT (4 copies)**

**Commander
Armed Services Technical Information Agency
Arlington Hall Station
Arlington 12, Virginia
Attn: TIPDR (10 copies)**

**National Bureau of Standards
Washington 25, D. C.
Attn: Library**

**Chief, Defense Atomic Support Agency
Washington 25, D. C.
Attn: DASARA
ATTN: DASATP
Attn: DASAAG/Library - 2 copies**

**Commander, Field Command
Defense Atomic Support Agency
Sandia Base
Albuquerque, New Mexico
Attn: FCWT
Attn: FCDR**

**Director, Advanced Research Projects Agency
Washington 25, D. C.
Attn: Chief, Tech Operations Div**

DISTRIBUTION (Continued)

Sandia Corporation
Sandia Base
Albuquerque, New Mexico
Attn: Dr. T. Cook
Attn: Dr. J. Easley
Attn: Mr. W. Snyder

Los Alamos Scientific Laboratory
Los Alamos, New Mexico
Attn: R. Watt/J-16

Ernest O. Lawrence Radiation Laboratory
Livermore, California
Attn: Library

U.S. Atomic Energy Commission
Germantown, Maryland
Attn: Div of Military Applications (DMA)

Bell Telephone Laboratories
Whippany, New Jersey
Attn: S. C. Rogers

Boeing Airplane Company
Seattle, Washington
Attn: Dr. D. Hicks

Bulova Research & Development Laboratories
Bulova Park
Flushing, Long Island, New York (Zone 70)
Attn: O. Brockmyer

CONVAIR
Division of General Dynamics Corporation
San Diego 12, California
Attn: Radiation Systems Section, R.E. Honer/J. Kluck

General Atomic Division General Dynamics
John Jay Hopkins Laboratory for Pure & Applied Science
San Diego 12, California
Attn: V.A.J. vanLint

General Electric Corporation
Electronics Laboratory
Syracuse, New York
Attn: Mr. J. Sinisgalli

Ministry of Supply Staff
British Joint Services Mission
3100 Massachusetts Ave., N. W.
Washington 8, D. C.
Attn: Reports Officer (2 copies)
Thru: Office, Chief of Ordnance, The Pentagon
Attn: ORDTN

DISTRIBUTION (Continued)

Hughes Aircraft Company
Research Laboratory
Culver City, California
Attn: T. D. Hanscome

International Business Machines Corporation
Owego, New York
Attn: R. Bohan

Radiation Effects Information Center
Battelle Memorial Institute
Columbus, Ohio

ORTISE
Box 62
Oak Ridge, Tennessee

Director, Office Special Weapons Development
USCONARC, Ft. Bliss, Texas

Senior Army Rocket & Guided Missile Agency Representative
Bell Telephone Laboratories
Whippany, New Jersey

Internal Distribution

Hinman, W.S., Jr./McEvoy, R. W.
Apstein, M./Gerwin, H.L./Guarino, P.A./Kalmus, H. P.
Fong, L.B.C./Schwenk, C.C.
Hardin, C. D., Lab 100
Horton, B. M., Lab 200
Rotkin, I., Lab 300
Landis, P. E./Tuccinardi, T. E., Lab 400
Hatcher, R. D., Lab 500
Flyer, I. N., Lab 600
Campagna, J. H./Apolenis, C. J., Div 700
DeMasi, R., Div 800
Franklin, P. J./Horse, E. F., Lab 900
Seaton, J. W./260
Mead, O. J., Jr., 210
Haas, P. H., 230 - 20 copies
Griffin, P. W., 240
Sommer, H., 250
Wimenitz, F. N., 230
Lackey, B. E., 230
Hoadley, J. C., 230
Rosenberg, J. D., 230
Caldwell, P. A., 230
Technical Reports Unit/800 (3 copies)
Technical Information Office, 010 (10 copies)
DOFL Library (5 copies)

(Two pages of abstract cards follow.)

UNCLASSIFIED

AD _____ Accession No. _____
 Diamond Ordnance Fuze Laboratories, Washington 25, D. C.
 NEUTRON DOSIMETRY USING INELASTIC SCATTERING THRESHOLD DETECTORS
 John S. Ingley

TR-905, 16 March 1961, 12 pp text, 14 pp illus. DA-5098-09-003,
 ONS-5010.11.83000, DOWL Proj 23320, UNCLASSIFIED Report

Employing a new threshold detector that utilizes the inelastic scattering reaction to the isomeric state of Ba^{137} , the time-integrated neutron flux above 1.9 Mev was measured in the General Atomic Triga reactor. The values compare favorably with those extrapolated from measurements of the flux above 2.9 Mev given by the standard sulfur pellet method, and evidence thus far indicates that the new method may provide a whole new series of threshold detectors.

Integrated neutron
 flux--
 Measurement of
 Threshold de-
 tectors
 Neutron dosim-
 try

Neutron dosimetry--
 Inelastic scat-
 tering method
 with threshold
 detectors

UNCLASSIFIED

AD _____ Accession No. _____
 Diamond Ordnance Fuze Laboratories, Washington 25, D. C.
 NEUTRON DOSIMETRY USING INELASTIC SCATTERING THRESHOLD DETECTORS
 John S. Ingley

TR-905, 16 March 1961, 12 pp text, 14 pp illus. DA-5098-09-003,
 ONS-5010.11.83000, DOWL Proj 23320, UNCLASSIFIED Report

Employing a new threshold detector that utilizes the inelastic scattering reaction to the isomeric state of Ba^{137} , the time-integrated neutron flux above 1.9 Mev was measured in the General Atomic Triga reactor. The values compare favorably with those extrapolated from measurements of the flux above 2.9 Mev given by the standard sulfur pellet method, and evidence thus far indicates that the new method may provide a whole new series of threshold detectors.

Integrated neutron
 flux--
 Measurement of
 Threshold de-
 tectors
 Neutron dosim-
 try

Neutron dosimetry--
 Inelastic scat-
 tering method
 with threshold
 detectors

UNCLASSIFIED

AD _____ Accession No. _____
 Diamond Ordnance Fuze Laboratories, Washington 25, D. C.
 NEUTRON DOSIMETRY USING INELASTIC SCATTERING THRESHOLD DETECTORS
 John S. Ingley

TR-905, 16 March 1961, 12 pp text, 14 pp illus. DA-5098-09-003,
 ONS-5010.11.83000, DOWL Proj 23320, UNCLASSIFIED Report

Employing a new threshold detector that utilizes the inelastic scattering reaction to the isomeric state of Ba^{137} , the time-integrated neutron flux above 1.9 Mev was measured in the General Atomic Triga reactor. The values compare favorably with those extrapolated from measurements of the flux above 2.9 Mev given by the standard sulfur pellet method, and evidence thus far indicates that the new method may provide a whole new series of threshold detectors.

Integrated neutron
 flux--
 Measurement of
 Threshold de-
 tectors
 Neutron dosim-
 try

Neutron dosimetry--
 Inelastic scat-
 tering method
 with threshold
 detectors

UNCLASSIFIED

AD _____ Accession No. _____
 Diamond Ordnance Fuze Laboratories, Washington 25, D. C.
 NEUTRON DOSIMETRY USING INELASTIC SCATTERING THRESHOLD DETECTORS
 John S. Ingley

TR-905, 16 March 1961, 12 pp text, 14 pp illus. DA-5098-09-003,
 ONS-5010.11.83000, DOWL Proj 23320, UNCLASSIFIED Report

Employing a new threshold detector that utilizes the inelastic scattering reaction to the isomeric state of Ba^{137} , the time-integrated neutron flux above 1.9 Mev was measured in the General Atomic Triga reactor. The values compare favorably with those extrapolated from measurements of the flux above 2.9 Mev given by the standard sulfur pellet method, and evidence thus far indicates that the new method may provide a whole new series of threshold detectors.

Integrated neutron
 flux--
 Measurement of
 Threshold de-
 tectors
 Neutron dosim-
 try

Neutron dosimetry--
 Inelastic scat-
 tering method
 with threshold
 detectors

REMOVAL OF EACH CARD WILL BE NOTED ON INSIDE EACH COVER, AND REMOVED
 CARDS WILL BE TREATED AS REQUIRED BY THEIR SECURITY CLASSIFICATION.

UNCLASSIFIED

AD _____ Accession No. _____
 Diamond Ordnance Fuze Laboratories, Washington 25, D. C.
 NEUTRON DOSIMETRY USING INELASTIC SCATTERING THRESHOLD DETECTORS
 John S. Ingley

TR-905, 16 March 1961, 12 pp text, 14 pp illus. DA-5898-09-003,
 ONS-5010.11.83000, DOWL Proj 23320, UNCLASSIFIED Report

Employing a new threshold detector that utilizes the inelastic scattering reaction to the isomeric state of Ba^{137} , the time-integrated neutron flux above 1.9 Mev was measured in the General Atomic Triga reactor. The values compare favorably with those extrapolated from measurements of the flux above 2.9 Mev given by the standard sulfur pellet method, and evidence thus far indicates that the new method may provide a whole new series of threshold detectors.

Integrated neutron flux--
 Measurement of Threshold detectors
 Neutron dosimetry

Neutron dosimetry--
 Inelastic scattering method with threshold detectors

AD

Accession No.

Diamond Ordnance Fuze Laboratories, Washington 25, D. C.

NEUTRON DOSIMETRY USING INELASTIC SCATTERING THRESHOLD DETECTORS
 John S. Ingley

TR-905, 16 March 1961, 12 pp text, 14 pp illus. DA-5898-09-003,
 ONS-5010.11.83000, DOWL Proj 23320, UNCLASSIFIED Report

Employing a new threshold detector that utilizes the inelastic scattering reaction to the isomeric state of Ba^{137} , the time-integrated neutron flux above 1.9 Mev was measured in the General Atomic Triga reactor. The values compare favorably with those extrapolated from measurements of the flux above 2.9 Mev given by the standard sulfur pellet method, and evidence thus far indicates that the new method may provide a whole new series of threshold detectors.

Integrated neutron flux--
 Measurement of Threshold detectors
 Neutron dosimetry

Neutron dosimetry--
 Inelastic scattering method with threshold detectors

UNCLASSIFIED

AD _____ Accession No. _____
 Diamond Ordnance Fuze Laboratories, Washington 25, D. C.
 NEUTRON DOSIMETRY USING INELASTIC SCATTERING THRESHOLD DETECTORS
 John S. Ingley

TR-905, 16 March 1961, 12 pp text, 14 pp illus. DA-5898-09-003,
 ONS-5010.11.83000, DOWL Proj 23320, UNCLASSIFIED Report

Employing a new threshold detector that utilizes the inelastic scattering reaction to the isomeric state of Ba^{137} , the time-integrated neutron flux above 1.9 Mev was measured in the General Atomic Triga reactor. The values compare favorably with those extrapolated from measurements of the flux above 2.9 Mev given by the standard sulfur pellet method, and evidence thus far indicates that the new method may provide a whole new series of threshold detectors.

Integrated neutron flux--
 Measurement of Threshold detectors
 Neutron dosimetry

Neutron dosimetry--
 Inelastic scattering method with threshold detectors

AD

Accession No.

Diamond Ordnance Fuze Laboratories, Washington 25, D. C.

NEUTRON DOSIMETRY USING INELASTIC SCATTERING THRESHOLD DETECTORS
 John S. Ingley

TR-905, 16 March 1961, 12 pp text, 14 pp illus. DA-5898-09-003,
 ONS-5010.11.83000, DOWL Proj 23320, UNCLASSIFIED Report

Employing a new threshold detector that utilizes the inelastic scattering reaction to the isomeric state of Ba^{137} , the time-integrated neutron flux above 1.9 Mev was measured in the General Atomic Triga reactor. The values compare favorably with those extrapolated from measurements of the flux above 2.9 Mev given by the standard sulfur pellet method, and evidence thus far indicates that the new method may provide a whole new series of threshold detectors.

Integrated neutron flux--
 Measurement of Threshold detectors
 Neutron dosimetry

Neutron dosimetry--
 Inelastic scattering method with threshold detectors

REMOVAL OF EACH CARD WILL BE NOTED ON INSIDE BACK COVER, AND REMOVED CARDS WILL BE TREATED AS REQUIRED BY THEIR SECURITY CLASSIFICATION.

UNCLASSIFIED

UNCLASSIFIED